Multigap superconductivity in locally noncentrosymmetric SrPtAs: An ^{75}As nuclear quadrupole resonance investigation

F. Brückner, R. Sarkar, M. Günther, H. Kühne, H. Luetkens, T. Neupert, A. P. Reyes, P. L. Kuhns, P. K. Biswas, T. Stürzer, D. Johrendt, and H.-H. Klauss

Phys. Rev. B **90**, 220503 — Published 1 December 2014

DOI: 10.1103/PhysRevB.90.220503

Multigap superconductivity in locally non-centrosymmetric SrPtAs: An ^{75}As nuclear quadrupole resonance investigation

F. Brückner,[1,*] R. Sarkar,[1] M. Günther,[1] H. Kühne,[2,3] H. Luetkens,[4] T. Neupert,[5] A. P. Reyes,[2] P. L. Kuhns,[2] P. K. Biswas,[4] T. Stürzer,[6] D. Johrendt,[6] and H.-H. Klauss[1]

[1]*Institute for Solid State Physics, TU Dresden, D-01069 Dresden, Germany*
[2]*National High Magnetic Field Laboratory, Florida State University, Tallahassee, Florida 32310, USA*
[3]*Dresden High Magnetic Field Laboratory (HLD), Helmholtz-Zentrum Dresden-Rossendorf, D-01314 Dresden, Germany*
[4]*Laboratory for Muon-Spin Spectroscopy, Paul Scherrer Institute, CH-5232 Villigen PSI, Switzerland*
[5]*Princeton Center for Theoretical Science, Princeton University, Princeton, New Jersey 08544, USA*
[6]*Department Chemie, Ludwig-Maximilians-Universität München, D-81377 Munich, Germany*

We report detailed ^{75}As-NQR investigations of the locally non-centrosymmetric superconductor SrPtAs. The spin-lattice relaxation studies prove weakly coupled multi-gap superconductivity. A retardation of the decay in $1/T_1T$ evidences a nodeless (fully gapped) superconducting state on the complex multi-pocket Fermi surface, which is consistent with an anisotropic s-wave order parameter and with proposed unconventional f-wave and chiral d-wave symmetries. A quantitative analysis of these models favors the unconventional f-wave state.

PACS numbers: 74.70.Xa, 74.25.nj, 76.60.Gv, 76.60.Es

I. INTRODUCTION

Since the discovery of superconductivity in doped transition metal pnictides in 2008,[1] this class of superconductors has grown to the largest family of superconductors with a common structural motive: They contain layers of square lattices formed by the transition metal elements. SrPtAs exhibits superconductivity below $T_c \approx 2.4$ K without doping, as recently found by Nishikubo et al.[2] SrPtAs crystallizes in a hexagonal structure of weakly coupled non-centrosymmetric PtAs-layers, in which the charge transport takes place. Adjacent PtAs-layers are inverted to each other, so that the bulk is indeed centrosymmetric. Thus, SrPtAs is a prime example for staggered non-centrosymmetricity.[3] A compound with a globally equivalent AlB_2-type structure, MgB_2, exhibits multigap superconductivity with $T_c \approx 40$ K.[4] The high spin-orbit coupling in SrPtAs opens the possibility for singlet-triplet mixing of the order parameter.[5] Interestingly, recent μSR experiments proved the development of a small static spontaneous internal field just below T_c, evidencing time reversal symmetry (TRS) breaking in superconducting SrPtAs.[6] This fact excludes a conventional superconducting state, that preserves TRS and can not coincide with an internal magnetic field. Different scenarios for this spontaneous TRS breaking are theoretically conceivable, all of which involve unconventional pairing states: The chiral d-wave superconducting state is particularly exciting, as it hosts striking topological phenomena such as chiral Majorana surface states and bulk Majorana Weyl nodes.[7] A second possibility is given by the f-wave symmetry,[8] that can break TRS symmetry at the surface.[6] Therefore, it is vital to understand the nature of the superconducting pairing in SrPtAs. In this context, nuclear magnetic resonance / nuclear quadrupole resonance (NMR/NQR) is one of the most powerful tools to shed light on such issues.

In this paper, we present ^{75}As-NQR investigations to determine the superconducting properties of SrPtAs. In the first stage of our experiments, ^{75}As-NMR experiments at 40 MHz were performed to extract the NQR frequency of SrPtAs in the normal metallic state, while a low upper critical field $H_{c2}(0)$ of approximately 2000 Oe does not allow NMR investigations in the superconducting phase. Therefore we carried out NQR experiments in a wide temperature range from 0.15 to 15 K. NQR experiments are performed in zero external static magnetic field. Since ^{75}As is a spin $I = 3/2$ nucleus, the NQR transitions ($\pm 1/2 \longleftrightarrow \pm 3/2$) result in a single line in the NQR spectrum. In addition to that, the nuclear magnetization recoveries are expected to exhibit a simple exponential form and a straightforward and unambiguous determination of the nuclear spin-lattice relaxation rate $1/T_1$ is possible. The temperature dependence of $1/T_1$ contains information about the symmetry of the superconducting order parameter.

Our main results are the evidence for multigap superconductivity with very weak inter-band coupling and constraints for the possible pairing symmetries. The Hebel-Slichter peak of $1/T_1T$ is strongly suppressed, but a strong displacement of the onset of the decay with respect to T_c evidences a fully gapped superconducting state – such as the theoretically predicted unconventional chiral d-wave or f-wave order parameter, that are both nodeless on the complex multi-pocket Fermi surface. In particular, the f-wave state is consistent to our data.

Parallel to our work, Matano et al.[9] performed NMR/NQR experiments on SrPtAs. While their ^{75}As T_1 relaxation data are consistent with ours with respect to the evidence for a fully gapped superconducting state. However, they did not observe a multigap behavior as shown in this work. In addition, we provide a deeper analysis and discussion in view of the published theoret-

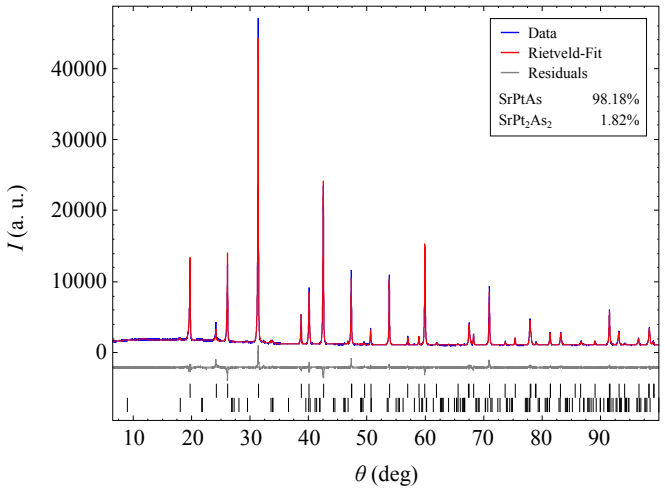

FIG. 1. X-ray powder diffraction plot of Sample B with Rietveld-fit. Two crystal phases are evident: SrPtAs (98.18 %) and $SrPt_2As_2$ (1.82 %). Stacking faults are regarded and are found to be minimal.

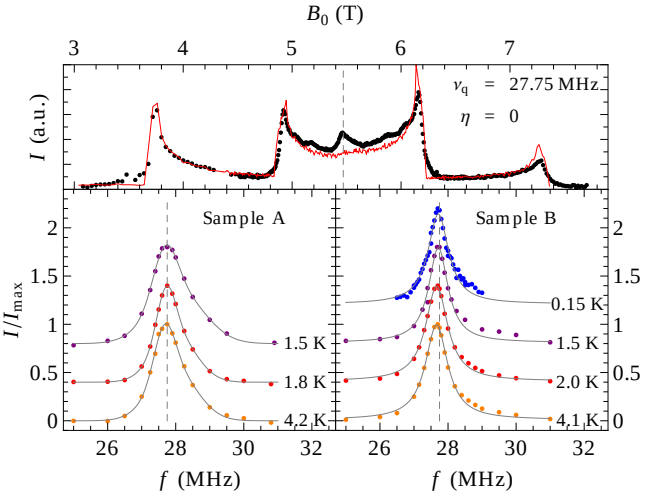

FIG. 2. Top: ^{75}As-NMR field sweep spectrum of sample A, recorded at 13 K and 40 MHz (black dots) versus the simulation graph (red line) as described in the text. The dotted vertical line indicates the ^{75}As-NMR Larmor field. Left lower panel: ^{75}As-NQR spectrum of sample A at three temperatures and double gaussian fit, right lower panel: ^{75}As-NQR spectrum of sample B with a lorentzian fit, vertical dashed line: $\nu_q = 27.75$ MHz.

ical work on SrPtAs which raised a large interest in this system. Note, that our T_1 data ranges to lower temperatures, where the multigap behavior is most significant.

II. BASIC NMR AND NQR PROPERTIES

Polycrystalline samples of SrPtAs were prepared via a solid state reaction method as described in Ref.[2]. Fig. 1 shows the angular dependence of X-ray diffraction on sample B. The major part (98.18 %) is pure SrPtAs. The Rietveld-fit comprises stacking faults that are found to be minimal. A second phase (1.82 %) is identified as the tetragonal $SrPt_2As_2$. NMR/NQR experiments were carried out with a pulsed spectrometer in dilution fridge, He-3 and He-4 cryostats. The spin-lattice relaxation time T_1 was measured by monitoring the nuclear magnetization recovery after a saturation radio frequency (RF) pulse at a frequency of $f = 27.75$ MHz both in the normal and superconducting state. Great care was taken in measuring $1/T_1$ to avoid possible RF heating at very low temperatures. We were able to exclude such effects by varying the repetition times between single measurements and comparing the relaxation rates (see Sec. III).

T_c of sample B is around 2.0 K, which has been estimated by *in situ* AC susceptibility (ACS) measurements by using the NMR coil. The results of the ACS measurements during cooling down and heating up the sample are plotted in the inset of Fig. 3.

Figure 2 (upper panel) shows the field sweep ^{75}As NMR spectrum at a fixed frequency of 40 MHz and $T = 13$ K. The spectrum represents a typical $I = 3/2$ nucleus in case of strong quadrupole interaction. To determine the ^{75}As-NQR frequency ν_q and the asymmetry parameter η, we diagonalized the nuclear Hamiltonian

$$H = -\gamma\hbar(\mathbf{B}_{ext}+\mathbf{B}_{hyp})\mathbf{I}+h\frac{\nu_q}{6}\left[3I_z^2-\mathbf{I}^2+\eta\left(I_x^2-I_y^2\right)\right] \quad (1)$$

at each sweep step for 25000 random orientations of the external field $\mathbf{B}_{ext}$ with respect to the electric field gradient (EFG) principle axis z. The best fitting quadrupole parameters are $\nu_q = 27.75$ MHz, $\eta = 0$ and no internal hyperfine field $\mathbf{B}_{hyp} = 0$ was found. Small additional intensity located near the center at around 5.5 T represents the $SrPt_2As_2$ phase. It shows a similar $I = 3/2$ spectrum with a quadrupolar fequency of $\nu_q \approx 5.4$ MHz. This crystallic phase does not disturb the NQR experiments that are taken around 27.75 MHz. Note that this value of the ^{75}As-NQR frequency in SrPtAs is much larger than in other transition metal pnictides[10,11].

Due to a very small upper critical field of approximately 2000 Oe, the irradiating pulse disturbs superconductivity. This effect manifests itself in a shift of the coil inductance. Therefore, the equilibrium superconducting state is not present while pulsing. However, the superconducting properties recover very fast on the μs timescale, which is small compared to the nuclear relaxation times. This is verified by measurements of the shift of the coil inductance after a strong pulse and is in line with the field cycle experiment described in Ref.[12], where the pulses are applied in the normal state. The effect on the relaxation experiments is discussed in section III.

Figure 2 (lower left panel, lower right panel) depicts several ^{75}As-NQR spectra recorded in the normal and in

the superconducting phase for the samples A and B. The NQR intensity was determined by integrating over the spin-echo signal, which gives a maximum of intenity but effects a small additional broadening. In the two regimes of the normal and superconducting state, the spectral shape does not change significantly, as well as ν_q is constant over the whole temperature range. The single peak structure rules out the presence of any spurious phases in SrPtAs with a nearby ν_q. A homogeneous signal is further supported by the fact, that the T_1 measurements at different positions in the NQR spectrum give equal T_1 values.

Sample A and sample B are of different quality, as deduced from the NQR spectra. Sample A yields a linewidth (FWHM) of ≈ 1 MHz, while sample B has a linewidth of ≈ 700 kHz. Both show a very slight asymmetry. This may be an effect of the crystal surface or impurities.

III. NUCLEAR RELAXATION RATE

The nuclear magnetization recovery curves were fitted by

$$m(t) = A\left(1 - B\ e^{-3\,t/T_1}\right), \qquad (2)$$

where $m(t)$ is the respective nuclear magnetization at a time t after the saturation pulse, A and B are parameters that determine scaling and an offset. The recovery curves could be described well by this single exponential function except in the superconducting regime, where a stretched exponential function $m(t) = A\{1 - B\ \exp(-(3\,t/T_1)^{\beta})\}$ is required. The stretching parameter β ranges from $\approx$0.5 at low temperatures $T < 400$ mK to ≈ 1 at $T > 1.2$ K. While the stretched exponential is commonly used when the intrinsic distribution of relaxation channels is broadened,[13] in this case it is found to be an experimental artefact: We found that β varies with the pulse power, and therefore relate this effect to the disturbance of superconductivity while pulsing. In fact a large scattering of β is observed, which proves that this is not an intrinsic effect. However, the characteristic T_1 is unaffected by β or the pulse power, which validates our experimental data. This is ensured by measurements with varied experimental parameters (in particular pulse power and duration), that show no deviation of T_1 with respect to the confidence interval. These test measurements were done at several temperatures.

In Fig. 3, the results of our ^{75}As NQR spin-lattice relaxation rate study are shown. While the presented data were taken at 27.75 MHz, data were also recorded at different frequencies to approve the constancy over the NQR spectrum. In the normal metallic state, $1/T_1T$ follows the simple Korringa relation ($T_1T = 0.97$ s K), as expected for SrPtAs.

The determination of T_c via ACS experiment (see inset of Fig. 3) reveals a critical temperature of ≈ 2.0 K, which

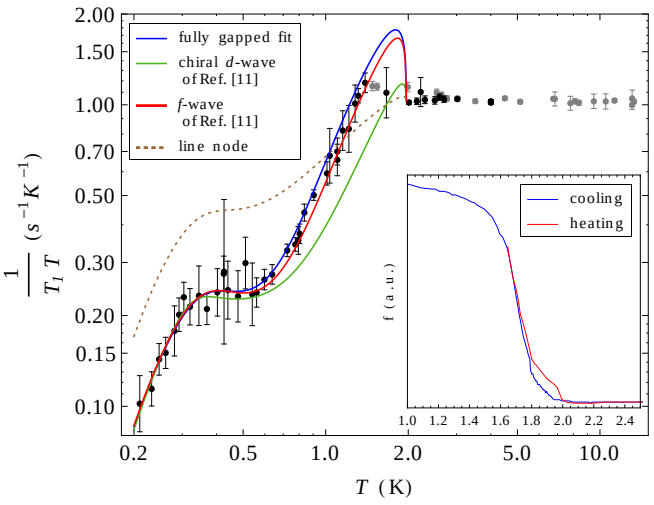

FIG. 3. ^{75}As spin-lattice relaxation rate: $1/T_1T$ versus temperature for sample B (black) and sample A (gray) with fits and simulations (see text). The hump at 300 mK indicates the opening of the second superconducting band. The fully gapped fit for the primarily superconducting band supports all proposed fully gapped states, including s-wave, chiral d-wave and f-wave gap. A line node model does not fit the data. The inset shows the temperature dependency of AC susceptibility data at zero field using the *in situ* NMR coil, revealing $T_c \approx 2.0$ K.

is in contrast to earlier findings of ≈ 2.4 K.[2,6] The discrepancy between T_c measured by means of ACS and the temperature, at which the spontaneous internal field developed in former μSR measurements, is not clear. Since it is the idem sample, it may be an effect of ageing but also may point to multiple phase transitions. The slow-onset increase of the resonance frequency might be due to a distribution of critical temperatures in the temperature interval from 1.8 K to 2.0 K. The hypothetically resulting distribution of relaxation times does not explain the above mentioned stretching of the exponential form of the relaxation recovery curves in a sufficient amount, it rather would have a minor effect that could only cause a stretching of $\beta \gtrsim 0.9$.

$1/T_1T$ shows a strong decrease below 1.3 K. The Hebel-Slichter peak is strongly suppressed in comparison with conventional s-wave superconductors. A second very distinct feature of the relaxation rate is a hump with a sharp edge at 300 mK. Below this edge, the relaxation rate obeys a power law decrease similar to the behavior near 1.3 K.

Earlier work on MgB_2 explains the suppression of a Hebel-Slichter peak with strong coupling effects or a possible quasiparticle broadening.[14] This is not necessarily adaptable to SrPtAs, in view of the smaller T_c, the broader peak and the rather sharp edge at 1.3 K. A distribution of critical temperatures might contribute to the suppression. However, a fully gapped superconducting state is probable. The hump at 300 mK indicates a

residual density of states (DOS) at the Fermi level, which suddenly disappears at 300 mK. This is explainable if one assumes multigap superconductivity with weak inter-band scattering (see below), which is in line with the suggestion of Nishikubo et al. for SrPtAs[2] based on the upward curvature of $H_{c2}(T)$.

The complex band structure of SrPtAs with three pairs of Fermi surfaces[15], the wealth of possible superconducting states and a corresponding large number of free parameters poses a challenge to the interpretation of $1/T_1$. One pair of Fermi surfaces, which hosts the largest density of states, is believed to drive the superconducting transition. Conventional s-wave as well as unconventional f-wave and chiral d-wave symmetries of the order parameter do not posses extended nodes on this pair of Fermi surfaces. Hence, a quantitative comparison of these possible pairing states is necessary. In the case of the f-wave symmetry, the nodes are placed in between the cylindrical Fermi surfaces centred around the K-point, which drive the superconductivity in SrPtAs. So the f-wave state is also fully gapped. Furthermore the f-wave pairing state is a triplet of the type $\sqrt{2}(\uparrow\downarrow + \downarrow\uparrow)$. Therefore this state can not be excluded by a suppressed Knight-shift in the superconducting phase found by Matano et al.[9] Indeed, in this compound, a Hebel-Slichter peak or a retardation of the decay in $1/T_1T$ does not imply conventional s-wave superconductivity. Furthermore, to eliminate line nodes in the order parameter, a corresponding model is included. All model functions are based on a generalized Hebel-Slichter formula (cf.[12]) for multigap characteristics and complex order parameters:

$$\frac{T_{1\mathrm{N}}}{T_{1\mathrm{S}}} = \frac{2}{k_{\mathrm{B}}T}\int_0^\infty \sum_{n=1,2} c_n \left[N_{\mathrm{s}}^n(E)^2 + M_{\mathrm{s}}^n(E)^2\right] \times f(E)(1-f(E'))dE, \quad (3)$$

with the density of states N_{s}, the so-called anomalous density of states M_{s}

$$\begin{aligned} N_{\mathrm{s}}^n(E) &= \Re\left[\int P_n(a)\frac{E}{\sqrt{E^2-|a|^2(\Delta_0^n)^2}}da\right] \\ M_{\mathrm{s}}^n(E) &= \Re\left[\int P_n(a)\frac{a\,\Delta_0^n}{\sqrt{E^2-|a|^2(\Delta_0^n)^2}}da\right], \end{aligned} \quad (4)$$

and the Fermi function f. The index n represents the number of the band and c_n determines the relative proportion of the density of states of band n. $P(a)$ is the distribution of the anisotropic superconducting gap $\Delta_n(\mathbf{\Omega}) = a(\mathbf{\Omega})\,\Delta_0^n$, where $\mathbf{\Omega}$ is the Fermi surface parametrization. $P(a) = \delta(a)$ describes the isotropic BCS case. This general multigap model implies that inter-band scattering of electrons during the relaxation process is suppressed, which is motivated by a very low inter-band coupling in multigap superconductors.

The temperature dependence of the superconducting gap is calculated by solving the BCS gap equation for multiple Fermi surfaces from[16] numerically for a specified T_{c} and then scaling the solution to obtain quotients $2\Delta_0/k_{\mathrm{B}}T_{\mathrm{c}}$ that differ from the BCS-result of 3.5.

The blue curve in Fig. 3 is calculated with a generic model: $P_n(a)$ is assumed to be a rectangular function, that is finite in the range $[1-\delta_n/2, 1+\delta_n/2]$. The anomalous density of states is finite, since $a > 1$. We set $T_{\mathrm{c}} = 2.0$ K, $\delta_1 = 0.36$, $\delta_2 = 0.8$, $c_1 = 0.85$ and $2\Delta_0^n/k_{\mathrm{B}}T_{\mathrm{c}} = 3.5$. Obviously, the pronounced Hebel-Slichter peak is not consistent with our data but the whole data at temperatures below 1.35 K are very well reproduced. Especially the hump structure at 0.3 K can be traced, which would not be possible when assuming a single gap. Thus a strong indication for multigap superconductivity is found. A commonly used interpretation of this model is an anisotropic (but conventional) s-wave symmetry, but also chiral d-wave and f-wave symmetry can lead to a similar behavior. As mentioned above, the overestimation of the Hebel-Slichter peak might be due to the distribution of critical temperatures, which would only lead to a small supression of the peak, or a temperature-dependence of the gap that differs from the BCS approximation. In both cases, the fitting parameters would change, but the essence remains: a fully gapped superconducting state with multiple gaps. According to the parameter c_1, the primarily superconducting band contains 71% of the total density of states $N(0)$. This is in general agreement with the LDA calculations,[15] that predict 74%.[5]

The line node order parameter produces a much flatter curve (see Fig. 3, brown curve) than our data and a rather instant decrease, which does not match to our findings. Since this behavior is due to line nodes in the gap function, we can generally exclude line nodes in the superconducting order parameter.

It is interesting how theoretical predictions, in particular for the chiral d-wave state[5,7] and the f-wave state[5,8], compare with the present NQR study. With the knowledge of the bandstructure and a simple representation of the chiral d-wave state and the f-wave state provided by Ref.[5], we calculated the spin-lattice relaxation rate without a variable fitting parameter for the anisotropy (in the previous model, this is the δ parameter). This is plotted in Fig. 3 (green/red line).

The chiral d-wave model clearly underestimates the relaxation rates, while the height of the Hebel-Slichter peak does agree with the data. For the secondary superconducting band we assumed an anisotropic s-wave symmetry as in the former fit. In contrast, the f-wave model does reproduce the data very well, similar to the general fully gapped fit. The reason for this behavior lies in the negligible scattering between the two disconnected Fermi surfaces related to the primarily superconducting band on one hand and in the narrower distribution of gaps on the other hand. Therefore the f-wave state is more suitable to explain our findings. Because the **k**-dependency of the gap function can differ significantly from the simple analytical representations we used for the fitting,[7] the

chiral d-wave state can not be excluded in general.

As pointed out in[7], the f-wave and chiral d-wave state are in competition to each other, where separated Fermi surfaces do rather lead to a dominant f-wave gap symmetry, while connected or nearby Fermi surfaces do favour the chiral d-wave state, driven by the van Hove singularities at the M-Point. With hole doping of SrPtAs it might be possible to connect the Fermi pockets near the van Hove singularities at the M-points, and find the distinct evidence of a chiral d-wave symmetry.

IV. CONCLUSION

Detailed ^{75}As-NQR investigations on two different polycrystalline samples of the locally noncentrosymmetric superconducting SrPtAs with $T_c \approx 2.0$ K are presented. In the normal state, $1/T_1T = const.$ is found as expected for metallic SrPtAs. The spin-lattice relaxation rate divided by temperature $1/T_1T$ shows a partly suppressed Hebel-Slichter peak and a hump structure around 300 mK, which refers to multigap superconductivity. Several fits and simulations were carried out to describe the $1/T_1T$ data. A fully gapped model fits to the observed decreasing behavior. In the case of SrPtAs, that includes also unconventional chiral d-wave and f-wave states. Especially the calculation of $1/T_1T$ using the f-wave gap symmetry does agree with our data. In establishing the multigap character of superconductivity in SrPtAs, our data provides guidance to revisit the theoretical models of the superconducting gap function, and constrains the possible pairing mechanisms.

ACKNOWLEDGMENTS

The presented experiments were performed at the Technische Universität Dresden, Germany, and at the National High Magnetic Field Laboratory USA, which is supported by National Science Foundation Cooperative Agreement No. DMR-1157490, the State of Florida, and the U.S. Department of Energy. Both samples were synthesized at the Ludwig-Maximilians-University Munich. We appreciate the support by the Deutsche Forschungsgemeinschaft through SA 2426/1-1, KU 3066/1-1 and the Research Training Group GRK 1621 at Technische Universität Dresden.

* fxbr.pc@gmail.com

[1] Y. Kamihara, T. Watanabe, M. Hirano, and H. Hosono, Journal of the American Chemical Society **130**, 3296 (2008).
[2] Y. Nishikubo, K. Kudo, and M. Nohara, Journal of the Physical Society of Japan **80**, 055002 (2011).
[3] M. H. Fischer, F. Loder, and M. Sigrist, Phys. Rev. B **84**, 184533 (2011).
[4] S. Souma, Y. Machida, T. Sato, T. T., M. H., S.-C. Wang, H. Ding, A. Kaminski, J. C. Campuzano, S. Sasaki, and K. Kadowaki, Nature **423**, 65 (2003).
[5] J. Goryo, M. H. Fischer, and M. Sigrist, Phys. Rev. B **86**, 100507 (2012).
[6] P. K. Biswas, H. Luetkens, T. Neupert, T. Stürzer, C. Baines, G. Pascua, A. P. Schnyder, M. H. Fischer, J. Goryo, M. R. Lees, H. Maeter, F. Brückner, H.-H. Klauss, M. Nicklas, P. J. Baker, A. D. Hillier, M. Sigrist, A. Amato, and D. Johrendt, Phys. Rev. B **87**, 180503 (2013).
[7] M. H. Fischer, T. Neupert, C. Platt, A. P. Schnyder, W. Hanke, J. Goryo, R. Thomale, and M. Sigrist, Phys. Rev. B **89**, 020509 (2014).
[8] W.-S. Wang, Y. Yang, and Q.-H. Wang, Phys. Rev. B **90**, 094514 (2014).
[9] K. Matano, K. Arima, S. Maeda, Y. Nishikubo, K. Kudo, M. Nohara, and G.-q. Zheng, Phys. Rev. B **89**, 140504 (2014).
[10] R. Sarkar, M. Baenitz, A. Jesche, C. Geibel, and F. Steglich, Journal of Physics: Condensed Matter **24**, 135602 (2012).
[11] R. Sarkar, R. Nath, P. Khuntia, H. S. Jeevan, P. Gegenwart, and M. Baenitz, Journal of Physics: Condensed Matter **24**, 045702 (2012).
[12] D. E. MacLaughlin, in *Solid State Physics*, Vol. 31 (Academic Press, 1976).
[13] F. Hammerath, U. Gräfe, T. Kühne, H. Kühne, P. L. Kuhns, A. P. Reyes, G. Lang, S. Wurmehl, B. Büchner, P. Carretta, and H.-J. Grafe, Phys. Rev. B **88**, 104503 (2013).
[14] H. Kotegawa, K. Ishida, Y. Kitaoka, T. Muranaka, and J. Akimitsu, Phys. Rev. Lett. **87**, 127001 (2001).
[15] S. J. Youn, M. H. Fischer, S. H. Rhim, M. Sigrist, and D. F. Agterberg, Phys. Rev. B **85**, 220505 (2012).
[16] H. Suhl, B. T. Matthias, and L. R. Walker, Phys. Rev. Lett. **3**, 552 (1959).
[17] Z. Li, D. L. Sun, C. T. Lin, Y. H. Su, J. P. Hu, and G.-q. Zheng, Phys. Rev. B **83**, 140506 (2011).
[18] G.-q. Zheng, K. Tanabe, T. Mito, S. Kawasaki, Y. Kitaoka, D. Aoki, Y. Haga, and Y. Onuki, Phys. Rev. Lett. **86**, 4664 (2001).
[19] S. Kawasaki, K. Shimada, G. F. Chen, J. L. Luo, N. L. Wang, and G.-q. Zheng, Phys. Rev. B **78**, 220506 (2008).
[20] K. Matano, Z. A. Ren, X. L. Dong, L. L. Sun, Z. X. Zhao, and G. qing Zheng, EPL (Europhysics Letters) **83**, 57001 (2008).
[21] V. A. Stenger, C. H. Pennington, D. R. Buffinger, and R. P. Ziebarth, Phys. Rev. Lett. **74**, 1649 (1995).
[22] D. Parker, O. V. Dolgov, M. M. Korshunov, A. A. Golubov, and I. I. Mazin, Phys. Rev. B **78**, 134524 (2008).
[23] J. Yang and G.-Q. Zheng, Mod. Phys. Lett. B **26**, 1230008 (2012).